



9th International Conference on Applied Energy, ICAE2017, 21-24 August 2017, Cardiff, UK

Effect of Thermal Cycling on Zinc Antimonide Thin Film Thermoelectric Characteristics

M. Mirhosseini¹, A. Rezania^{1,*}, L. Rosendahl¹, Bo B. Iversen²

¹Department of Energy Technology, Aalborg University, Pontoppidanstraede 111, 9220 Aalborg East, Denmark

²Centre for Materials Crystallography, Department of Chemistry and iNANO, Aarhus University, Langelandsgade 140, DK-8000 Aarhus C, Denmark

Abstract

In this study, performance and stability of zinc antimonide thin film thermoelectric sample is analyzed under transient thermal conditions. The thermoelectric materials are deposited on glass based substrate where the heat flow is parallel with the thermoelectric element length. The specimen is fixed between a heater block and heat sink cooled by the ambient. The thermoelectric element is studied under open circuit and also optimal constant loads corresponding to maximum power output. The thermal cycles are provided for five different hot junction temperatures, 160, 200, 250, 300 and 350 °C. The results show that the thin film has high reliability after thermal and electrical cycles, and no performance degradation is observed.

© 2017 The Authors. Published by Elsevier Ltd.

Peer-review under responsibility of the scientific committee of the 9th International Conference on Applied Energy.

Keywords: Thin Film TEG; Thermal Cycling; Zinc Antimonide; Transient Behavior; Energy Generation.

1. Introduction

Thermoelectric (TE) devices have been employed for many years as a reliable energy conversion technology for applications ranging from the cooling devices to the direct conversion of heat into electricity for power generation. The efficiency of TE materials is evaluated using the dimensionless figure of merit, $zT = \alpha^2 T / (\rho \kappa)$, where α is the Seebeck coefficient, T is absolute temperature, ρ is electrical resistivity, and κ is the total thermal conductivity consisting of contribution from the charge carrier κ_e and the lattice κ_l [1]. Although most researches concern bulk materials for high power applications such as recovery of waste heat from car exhaust, attractive low power applications of thin films are evident. The inherent phonon scattering due to the nanostructure of the thin films can enhance TE properties [2]. As a new kind of environmentally friendly material, Zn-Sb is made of relatively cheap and nontoxic elements. The Zn-Sb binary system contains ZnSb and β -Zn₄Sb₃, which are promising p-type TE materials for low cost thermoelectric application, intended to operate at intermediate temperatures (from room temperature up to 350 °C) [3].

* Corresponding author. Tel.: +45-9940-9276; fax: +45-9815-1411.
E-mail address: alr@et.aau.dk

Thin film technique is a promising method for improving the thermoelectric properties of TE material due to low dimensional quantum confinement and a much lower lattice thermal conductivity [4]. The improvement of the properties of the thin film TE materials has introduced a huge potential in application of miniaturization sensors, micro-power source and other thermoelectric applications of the thin film TE devices. Furthermore, in some applications of micro scale TE devices, thin films are very required [5]. In a conceptual design, one way to produce more electrical power by using thin film based thermoelectric module, is that heat flow runs parallel to the surface of thin films deposited on an insulating substrate. Fan et al. [6] demonstrated the properties of their designed thin film thermoelectric generators with heat flow running in longitudinal direction of the film, where the maximum temperature difference between both sides is maintained 85 °C. N-type Bi₂Te₃ and p-type Sb₂Te₃ thin films were deposited on soda-lime glass substrates. They argued that the performance of thin film TEG with this structure can be further improved by optimization of TE materials and fabrication methods. In other study reported by Fan et al. [7], a promising flexible thin film thermoelectric generator using the n-type Al-doped ZnO and p-type Zn-Sb based thin film was demonstrated. The cold side was fixed at 300 K and the hot side was heated by an electrical stove to reach fixed temperatures. By increasing the hot side temperature, the output voltage of the p-n junction increased. When the temperature reached to 503 K, the output voltage had its max value. Although, when the hot side temperature exceeds 508 K, the output voltage rapidly decreased. Therefore, the suggested flexible substrate used in their work should be used for under 520 K applications. When the temperature increases further, the flexible substrate will be metamorphosed and the thermal stress across the thin film thermoelectric and the substrate will be increased, which causes the electrode fall off or the contact become loose. Only these two recent articles discussed about the thermoelectric properties of thin film samples in the longitudinal direction parallel to the heat flow by using constant hot side temperatures when the cold side is exposed to the environmental temperature. According to fundamental investigations to analyse the characteristics and behaviour of the uni-thin film done by few studies on the thermoelectric properties of thin film samples in the longitudinal direction parallel to the heat flow, an efficient thin film TEG module based on p-n couples can be designed and fabricated. Therefore, in the present study a zinc antimonide thin film sample is tested under different thermal and electrical load conditions. For this purpose, the sample is mounted between two blocks; hot side and cold side; whereas the cold side block is exposed to the environmental temperature (about 30 °C) and the hot side block contacts to a heater. The heat flow runs parallel to the surface of thin films sample. Since, operating conditions could be transient in practice; thermoelectric behaviour analysis is evaluated in transient condition as well as steady state. Thermal cycling is a way to expose the sample to different thermal conditions. Different maximum temperatures on the hot side are provided by cyclic manner; 160, 200, 250, 300 and 350 °C, for each experiment. Two scenarios are applied to test the sample in the presence of thermal cycling: without electrical load (open circuit), with constant electrical load corresponding to obtain maximum output power in aimed temperatures.

2. Experimental apparatus and procedure

2.1. Thin film production

A thin film sample has been manufactured by magnetron co-sputtering deposition in Aarhus University, Denmark. The Zn-Sb film was deposited directly on fused silica substrate. One target was a commercial Zn-target, whereas the other was produced in-house by the process reported by Yin et al. [8]. The substrate is a 350 µm thick single-sided polished fused silica wafer. The film thickness is about 600 nm, which was measured from the cross sectional SEM image. Before and after the annealing treatment, change of the film thickness was not observed. This sample has been produced with atomic ratio (Zn:Sb) equal to 57.6:42.4. This is roughly the same as for the Zn-Sb film declared by Sun et al. [9]. XRD pattern for the specimen is shown in Fig. 1. The ratio of ZnSb: Zn₄Sb₃ is about 6:4; therefore, the dominant phase is ZnSb. The photographs of the sample are shown in Fig. 2. As observed in Fig. 2-b, the specimen is a rectangular thin film by the length and width equal to 19.8 and 17.2 mm, respectively. The length of hot side and cold side contact area is 3 mm that is subtracted from the total length for obtaining the effective length.

2.2. Thin film test bench

The test device integrated on the Bench (Fig. 3) with capability of heating the hot side up to 400 °C. This equipment is designed and developed to test coated thin film TE specimens and TE single legs. The cold side of the sample is only in contact with cold side thin block with natural convection cooling during the test. The temperature of the hot side can be adjusted between 150 °C and 400 °C. Hot side and cold side temperatures are measured by thermocouples mounted on both sides of the sample. Probes for voltage measurement are settled under the screws, first one connected to the hot side of the sample and the second one connected to the cold side (Fig. 2-a).

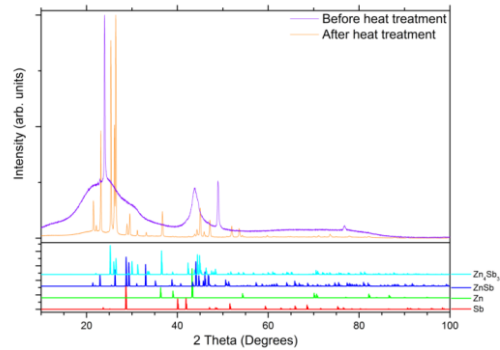


Fig.1: XRD patterns of Zn-Sb thin film

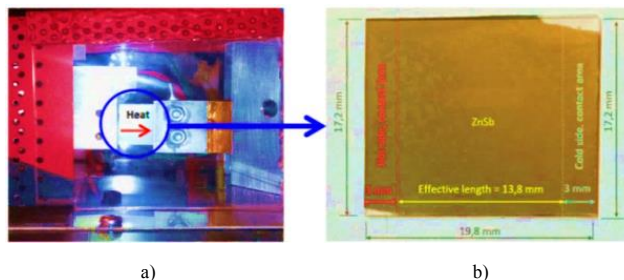


Fig.2: Photographs of the sample; a) the sample mounted between the hot side (left) and cold side (right) blocks; b) Geometric parameters of the sample

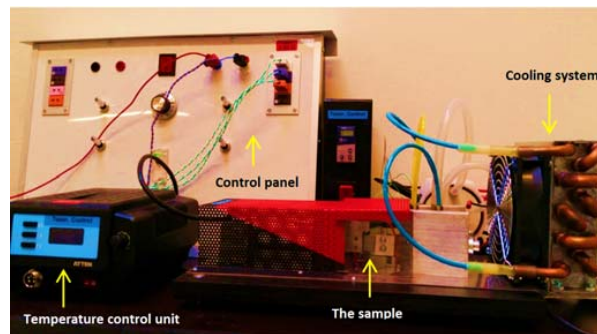


Fig.3: Experimental apparatus

3. Results and discussions

Thermal cycling (with/without electrical load) can show us how the important parameters change by increasing or decreasing temperature; whether these data are reliable and reproducible in the range of permitted standard deviation and with enough accuracy or not. Herein, to investigate characteristics and stability of the sample as thermoelectrically, hot side temperature, voltage, and Seebeck coefficient are parameters which are shown for open circuit analysis. Also, the hot side temperature, voltage, current, power are parameters which are presented for closed circuit analysis. Interval time of measurements is considered to be 15 seconds.

3.1. Thermal cycling without load

In this subsection, thermoelectric behavior of the sample is investigated by thermal cycling without applying load resistance. Ten thermal cycles are applied in order to evaluating repeatability of the results, and to show the sample's performance consistency in operating conditions. In Fig. 4-a, hot side temperature of the sample during the time is shown. To form the thermal cycling, the heater switching time is adjustable by a relay mounted on the control panel of the test bench. In this study, time of the heating and cooling for all experiments is 8 minutes. Generally, temperature distribution is transient at the beginning of the heating stage in each cycle until the thin film temperature distribution reaches equilibrium, before the cooling stage starts. As shown in Fig. 4-

b, voltage follows same trend as the hot side temperature during the cycles. The values of current and, accordingly, power during this part of experiments are zero, due to the open circuit condition. Using the hot and cold side temperatures and the voltage to calculate instantaneous Seebeck coefficient shows an interesting trend of the Seebeck coefficient in both of the steady state and transient condition. Nevertheless, definition of Seebeck coefficient can be applied also in transient conditions; under such conditions where it can be named as transient Seebeck coefficient. Variation of the Seebeck coefficient with respect to time is shown in Fig. 4-c. By tracking the data in this figure, constant variation of the data points represents steady state condition. A part of a few data points at the beginning of the heating stage which is for switching on moments of the heater, the rate of increasing the temperature difference is higher than increasing the voltage and the value of local Seebeck coefficient is alleviated to reach its steady state values. In the cooling stage, the rate of degradation of the temperature difference is less than decreasing the voltage and the value of local Seebeck coefficient is again reduced. In steady state period, these data values are close to each other during the tests in spite of different thermal conditions. In this figure and also in figures of subsection 3.2, lower and upper bounds of the data have been drawn by using calculated standard deviation (average value \pm standard deviation).

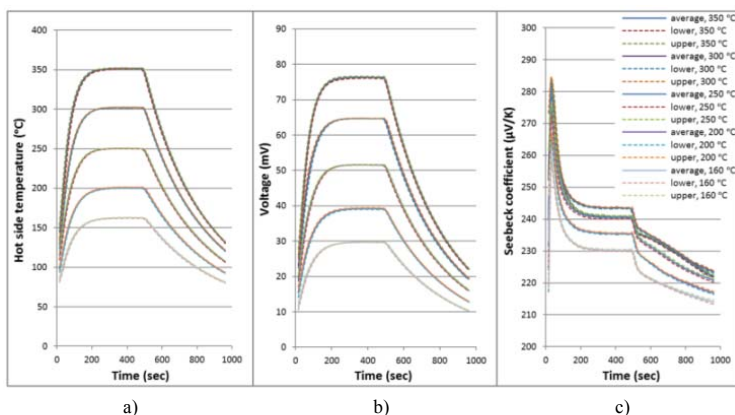


Fig.4: Variation of a) hot side temperature, b) voltage and c) Seebeck coefficient with time

Voltage versus temperature difference ($\Delta T = T_{hot} - T_{cold}$) is shown for different aimed hot side temperatures in Fig. 5. The trend of the data sets is similar to each other for all cases, showing that the voltage is increasing by rising the temperature difference and vice versa. During the transient state, there is not a single voltage data point for each temperature difference in different boundary conditions and even in heating and cooling period of a cycle. It is due to several parameters such as thermal diffusivity and hysteresis effect which can change by various parameters. The magnitude of hysteresis is a function of thickness, particle size, rate of heating or cooling, and impurities of the sample [10]. For each data set, the voltage data points in transient condition are dispersed, while the data points related to the steady state condition are obviously aggregated. The voltage corresponding to steady state in each data set (at the end of the heating stage) has been displayed in the circle in Fig. 5. In Fig. 6, the Seebeck coefficient versus average temperature of the sample is observed for all cycles. The Seebeck coefficient in steady state condition (inside the circle) increases up to a maximum value and then decreases by raising the hot side temperature. The bipolar effect is the main reason of reducing the Seebeck coefficients from hot side temperature 300 °C to 350 °C. Bipolar transport effect has been reported for zinc antimonide in the study done by Xiong et al. [11]. The maximum value of α in steady state was obtained 244 $\mu V/K$ as it is seen in Fig. 6.

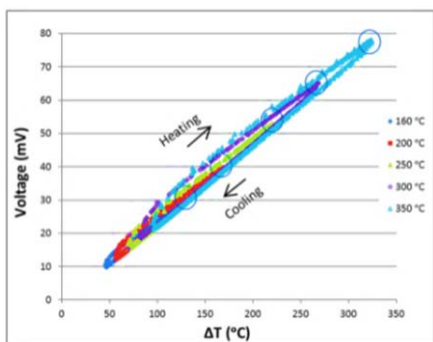


Fig.5: Voltage versus temperature difference

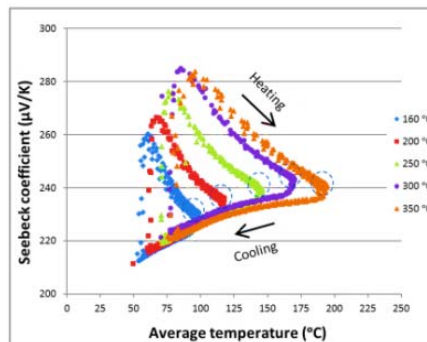


Fig.6: Seebeck coefficient versus average temperature of the sample

3.2. Thermal cycling with constant load corresponding to peak power point (PPP)

A wide range of load resistance (from 10 to 300 Ω) was firstly applied to find optimal electrical load value giving the maximum power generation by the thin film sample. The obtained load resistance is shown to be a function of temperature (Table 1). In each aimed temperature, the individual load corresponding to PPP is implemented.

Table 1: Load resistances corresponding to PPP by considering contact resistance

Hot side temperature [$^{\circ}\text{C}$]	160	200	250	300	350
Load resistance (at PPP) [Ω]	188.01	186.51	182.63	181.85	170.25

In this part, from the start point of the thermal cycles, the load is applied and continues to the end of that experiment. As shown in Fig. 7, the behavior of voltage, current and power is exactly congruous to the hot side temperature versus time.

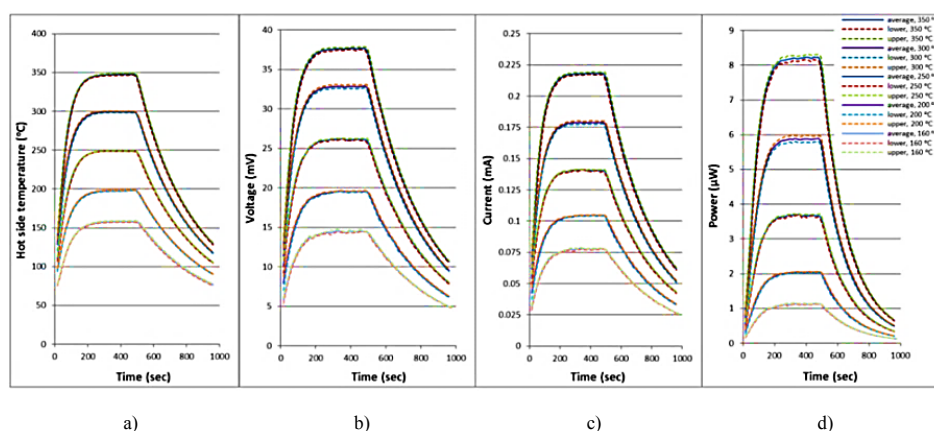


Fig. 7: Results for constant load over cycles, a) Hot side temperature, b) Voltage, c) Current, d) Power

4. Conclusions

Behaviour of thin film Zn-Sb sample in transient and steady state is investigated, as the heat transfer is in longitudinal direction of the sample. In the open circuit analysis, using hot and cold side temperatures and voltage to calculate instantaneous Seebeck coefficient showed transient trend of the Seebeck coefficient during the thermal cycling. An increase in Seebeck coefficient by increasing the hot side temperature was observed, although for more than 300 $^{\circ}\text{C}$, the Seebeck coefficient decreased due to the bipolar transport effect. The energy production by applying load in heating stages is about 70% of total energy producible by applying the same load among the whole domain of thermal cycles, whereas it will be about 30% if only the cooling stages are used for producing energy. The results showed the data are reliable and reproducible with permissive standard deviation and enough accuracy. One important message of this work could be that there is no need to have an efficient heat sink if the thin film element is used longitudinally. Furthermore, the thin film sample represented that can operate in relatively different ranges of temperature and load with long operation period without failure.

Acknowledgments

This work was carried out within the framework of the Center for Thermoelectric Energy Conversion (CTEC) and is funded in part by the Danish Council for Strategic Research, Programme Commission on Energy and Environment, under Grant No. 1305-00002B. The authors wish to thank Mr Anders Bank Blichfeld, PhD, in Centre for Materials Crystallography, Department of Chemistry and iNANO, Aarhus University, due to his support for producing the sample.

References

- [1] Snyder GJ, Toberer ES, Complex thermoelectric materials. *Nat Mater* 2008; 7:105-114.
- [2] Vineis CJ, Shakouri A, Majumdar A, Kanatzidis MG, Nanostructured thermoelectrics: big efficiency gains from small features. *Adv Mater* 2010; 22:3970-3980
- [3] Zheng ZH, Fan P, Liu PJ, Luo JT, Cai XM, Liang GX, Zhang DP, Ye F, Li YZ, Lin QY, Enhanced thermoelectric properties of mixed zinc antimonide thin films via phase optimization. *Appl Surf Sci*. 2014; 292:823-827

- [4] Ohta H, Kim SW, Mune Y, Mizoguchi T, Nomura K, Ohta S, Nomura T, Nakanishi Y, Ikuhara Y, Hirano M, Hosono H, Koumoto K, Giant thermoelectric Seebeck coefficient of a two-dimensional electron gas in SrTiO₃. *Nat Mater* 2007; 6:129-134
- [5] Fan P, Fan WF, Zheng ZH, Zhang Y, Luo JT, Liang GX, Zhang DP, Thermoelectric properties of zinc antimonide thin film deposited on flexible polyimide substrate by RF magnetron sputtering. *J Mater Sci: Mat. Electron* 2014; 25:5060-5065
- [6] Fan P, Zheng ZH, Cai ZK, Chen TB, Liu PJ, Cai XM, Zhang DP, Liang GX, Luo JT, The high performance of a thin film thermoelectric generator with heat flow running parallel to film surface. *Appl Phys Lett* 2013; 102:033904
- [7] Fan P, Zheng ZH, Li YZ, Lin QY, Luo JT, Liang GX, Cai XM, Zhang D, Ye F, Low-cost flexible thin film thermoelectric generator on zinc based thermoelectric materials. *Appl Phys Lett* 2015; 106:073901
- [8] Yin H, Blichfeld AB, Christensen M, Iversen BB, Fast direct synthesis and compaction of homogenous phase-pure thermoelectric Zn₄Sb₃. *ACS Appl Mater Interfaces* 2014; 6:10542-10548
- [9] Sun Y, Christensen M, Johnsen S, Nong NV, Ma Y, Sillassen M, Zhang E, Palmqvist AEC, Böttiger J, Iversen BB, Low-cost high-performance zinc antimonide thin films for thermoelectric applications. *Adv Mater* 2012; 24:1693-1696
- [10] Das VD, Karunakaran D, Thermal hysteresis during phase transition in Ag₂Te thin films: Thickness effect. *J Appl Phys* 1989; 66:1822-1825
- [11] Xiong DB, Okamoto NL, Inui H, Enhanced thermoelectric figure of merit in p-type Ag-doped ZnSb nanostructured with Ag₃Sb. *Scripta Materialia* 2013; 69:397-400